

(4)

2116 FILE COPY

AD-A207 759

TECHNICAL REPORT BRL-TR-2998

**BRL**

COLLISIONAL TRANSFER BETWEEN AND QUENCHING  
OF THE  $3P^3P$  AND  $5P$  STATES  
OF THE OXYGEN ATOM

**DTIC**  
**ELECTE**  
**MAY 16 1989**  
**S D**

BRAD E. FORCH  
ANDRZEJ W. MIZIOLEK  
PAUL J. DAGDIGIAN

MAY 1989

APPROVED FOR PUBLIC RELEASE; DISTRIBUTION UNLIMITED.

U.S. ARMY LABORATORY COMMAND

BALLISTIC RESEARCH LABORATORY  
ABERDEEN PROVING GROUND, MARYLAND

89 5 15 055

UNCLASSIFIED

SECURITY CLASSIFICATION OF THIS PAGE

| REPORT DOCUMENTATION PAGE   |       |  |   | Form Approved<br>OMB No. 0704-0188    |                                  |
|---|-------|--|---|---------------------------------------|----------------------------------|
| 1a. REPORT SECURITY CLASSIFICATION<br>Unclassified  |       |  | 1b. RESTRICTIVE MARKINGS  |                                       |                                  |
| 2a. SECURITY CLASSIFICATION AUTHORITY   |       |  | 3. DISTRIBUTION/AVAILABILITY OF REPORT<br>APPROVED FOR PUBLIC RELEASE; DISTRIBUTION UNLIMITED |                                       |                                  |
| 2b. DECLASSIFICATION/DOWNGRADING SCHEDULE   |       |  |   |                                       |                                  |
| 4. PERFORMING ORGANIZATION REPORT NUMBER(S)<br>BRL-TR-2998  |       |  | 5. MONITORING ORGANIZATION REPORT NUMBER(S)   |                                       |                                  |
| 6a. NAME OF PERFORMING ORGANIZATION<br>US Army Ballistic Research Laboratory  |       | 6b. OFFICE SYMBOL<br>(If applicable)<br>SLCRR-IB | 7a. NAME OF MONITORING ORGANIZATION   |                                       |                                  |
| 6c. ADDRESS (City, State, and ZIP Code)<br>Aberdeen Proving Ground, MD 21005-5066   |       |  | 7b. ADDRESS (City, State, and ZIP Code)   |                                       |                                  |
| 8a. NAME OF FUNDING/SPONSORING ORGANIZATION   |       | 8b. OFFICE SYMBOL<br>(If applicable)             | 9. PROCUREMENT INSTRUMENT IDENTIFICATION NUMBER   |                                       |                                  |
| 8c. ADDRESS (City, State, and ZIP Code)   |       |  | 10. SOURCE OF FUNDING NUMBERS   |                                       |                                  |
|   |       |  | PROGRAM ELEMENT NO.<br>61102A   | PROJECT NO.<br>AH43                   | TASK NO.                         |
|   |       |  | WORK UNIT ACCESSION NO.   |                                       |                                  |
| 11. TITLE (Include Security Classification)<br>COLLISIONAL TRANSFER BETWEEN AND QUENCHING OF THE $3p^3P$ AND $5p^5P$ STATES OF THE OXYGEN ATOM  |       |  |   |                                       |                                  |
| 12. PERSONAL AUTHOR(S)<br>Paul J. Dagdigian*, Brad E. Forch, Andrzej W. Miziolek  |       |  |   |                                       |                                  |
| 13a. TYPE OF REPORT<br>Final  |       | 13b. TIME COVERED<br>FROM Oct 87 TO Sep 88       |   | 14. DATE OF REPORT (Year, Month, Day) |                                  |
| 15. PAGE COUNT  |       |  |   |                                       |                                  |
| 16. SUPPLEMENTARY NOTATION<br>*The Johns Hopkins University<br>Published in Chemical Physics Letters  |       |  |   |                                       |                                  |
| 17. COSATI CODES  |       |  | 18. SUBJECT TERMS (Continue on reverse if necessary and identify by block number)             |                                       |                                  |
| FIELD   | GROUP | SUB-GROUP  | Excitation Transfer, Oxygen Atoms, Quenching, Two-Photon Fluorescence, Nitrogen. (mgn)        |                                       |                                  |
| 20  | 05    |  |   |                                       |                                  |
| 21  | 02    |  |   |                                       |                                  |
| 19. ABSTRACT (Continue on reverse if necessary and identify by block number)<br>Collisional quenching and excitation transfer between the oxygen atom $3p^3P$ and $5p^5P$ states have been investigated in a discharge flow apparatus with $O_2^+$ and $N_2$ collisional partners. The $3p^3P$ state was excited by two-photon excitation at 225.6 nm from the $2p^4^3P$ ground state, and temporal profiles of the $3p^3P$ and $5p^5P$ emission at 844.7 and 777.5 nm, respectively, to the lower $3s$ manifold were recorded. From an analysis of $3p^3P$ decay curves as a function of quencher pressure, the following bimolecular rate constants for the removal of the $3p^3P$ state were determined: $k_3^O(O_2) = (7.8 \pm 0.8) \times 10^{-10}$ and $k_3^O(N_2) = (5.87 \pm 0.15) \times 10^{-10}$ molecule $^{-1}$ cm $^3$ s $^{-1}$ . The intercept of the $O_2$ Stern-Vollmer plot yielded $k_3^r = (2.98 \pm 0.15) \times 10^7$ s $^{-1}$ for the $3p^3P$ radiative decay rate. The collisional quenching rate constant for the $5p^5P$ state by $O_2$ was obtained by analysis of $5p^5P$ decay curves: $k_5^O(O_2) = (10.8 \pm 1.8) \times 10^{-10}$ molecule $^{-1}$ cm $^3$ s $^{-1}$ . Rate constants $k_{35}$ for $3p^3P \rightarrow 5p^5P$ excitation transfer were obtained from measurements of the ratio of the $5p^5P$ to $3p^3P$ emission intensities as a function of |       |  |   |                                       |                                  |
| 20. DISTRIBUTION/AVAILABILITY OF ABSTRACT<br><input type="checkbox"/> UNCLASSIFIED/UNLIMITED <input checked="" type="checkbox"/> SAME AS RPT. <input type="checkbox"/> DTIC USERS   |       |  | 21. ABSTRACT SECURITY CLASSIFICATION<br>Unclassified  |                                       |                                  |
| 22a. NAME OF RESPONSIBLE INDIVIDUAL<br>DR. ANDRZEJ W. MIZIOLEK  |       |  | 22b. TELEPHONE (Include Area Code)<br>301-278-6157  |                                       | 22c. OFFICE SYMBOL<br>SLCRR-IB-I |

DD Form 1473, JUN 86

Previous editions are obsolete.

SECURITY CLASSIFICATION OF THIS PAGE

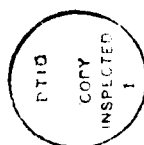
UNCLASSIFIED

19. Abstract (Cont'd):

quencher pressure. We find  $k_{35}(\text{O}_2) \approx 6 \times 10^{-11}$  and  $k_{35}(\text{N}_2) \approx 2 \times 10^{-11}$  molecule<sup>-1</sup> cm<sup>3</sup> s<sup>-1</sup>. These measurements are important for quantitative determination of oxygen atoms in combustion environments and for multiphoton photochemical ignition of reactive gases which involve oxygen-atom two-photon transitions at 225.6 nm.

# TABLE OF CONTENTS

|  | <u>Page</u> |
|--|-------------|
| LIST OF FIGURES.....                   | 5           |
| I. INTRODUCTION.....                   | 7           |
| II. EXPERIMENTAL.....                  | 9           |
| III. RESULTS.....                      | 10          |
| A. Fluorescence Waveforms.....         | 10          |
| B. Kinetic Equations.....              | 12          |
| C. Quenching Rate Constants.....       | 13          |
| D. Energy Transfer Rate Constants..... | 15          |
| IV. DISCUSSION.....                    | 18          |
| ACKNOWLEDGEMENT.....                   | 21          |
| REFERENCES.....                        | 23          |
| DISTRIBUTION LIST.....                 | 25          |



|                    |                                     |
|--------------------|-------------------------------------|
| Accession For      |                                     |
| NTIS CRA&I         | <input checked="" type="checkbox"/> |
| DTIC TAB           | <input type="checkbox"/>            |
| Unannounced        | <input type="checkbox"/>            |
| Justification      |                                     |
| By                 |                                     |
| Distribution/      |                                     |
| Availability Codes |                                     |
| Dist               | Avail and/or Special                |
| A-1                |                                     |

# LIST OF FIGURES

| <u>Figure</u> |  | <u>Page</u> |
|---------------|--|-------------|
| 1             | Relevant Energy Levels for Two-Photon Excitation of Oxygen Atoms and Excited-State Collisional Energy Transfer.....  | 8           |
| 2             | Schematic Diagram of the Experimental Apparatus.....   | 9           |
| 3             | Waveforms for (a) the $3p + 3S$ and (b) the $5p + 3S$ Fluorescence Emission Upon Two-Photon Excitation of the $3p\ 3P$ State.....                              | 11          |
| 4             | Stern-Volmer Plots for (a) the $3p + 3S$ Emission at 844.7 nm and (b) the $5p + 5S$ Emission at 777.5 nm as a Function of $O_2$ Quencher Partial Pressure..... | 14          |
| 5             | Ratio of the Integrated $5p + 5S$ to $3p + 3S$ Emission Intensity Versus added (a) $O_2$ and (b) $N_2$ .....   | 16          |

## I. INTRODUCTION

There is a considerable need for well-characterized diagnostic techniques for the quantitative measurement of the concentrations of species in propellant flames and other combustion environments. The use of multiphoton excitation schemes for the detection of light atoms, such as oxygen, has drawn considerable interest in recent years.<sup>1-12</sup> Two different approaches have been employed in these methods, namely observation of the fluorescence emission from the multiphoton-excited resonant state<sup>1-8</sup> or absorption of an additional photon to produce ionization.<sup>8-12</sup> Both of these schemes have been utilized for the detection of hydrogen and oxygen atoms in flames. The former method has advantages over the latter in that it does not require the insertion of a probe into the medium and can also be used to obtain two-dimensional images of atomic concentrations in flames, as has recently been demonstrated.<sup>13,14</sup> It is also easier to discriminate against background photon emission than ionization.

Figure 1 illustrates the scheme which has been used for the detection of oxygen atoms.<sup>1,3,5,6,8,13,14</sup> Here, oxygen atoms are excited in a two-photon transition to the  $3p\ ^3P$  state with 225.6 nm laser radiation and are detected by observation of the fluorescent emission to the  $3s\ ^3S$  state at 844.7 nm. A number of parameters are required for the use of this diagnostic tool in a quantitative fashion. Recently, Bamford, et al.,<sup>8</sup> have reported absolute cross sections for the two-photon absorption process, as well as for one-photon photoionization of the  $3p$  state. Bimolecular collision quenching rate constants for this state have also been measured by several groups.<sup>1,6,8</sup> These data are required to account for collisional effects in finite-pressure environments.

Miziolek and DeWilde<sup>5</sup> have also shown the potential importance of collisional excitation transfer processes in the collisional removal of this highly excited atomic state. They excited oxygen atoms by two-photon absorption at 225.6 nm in an atmosphere-pressure  $CH_4-N_2O-N_2$  flame and observed within and through the flame front not only  $3p \rightarrow 3s$  emission at 844.7 nm, but also  $5p \rightarrow 5s$  emission of even greater intensity at 777.5 nm. Similar detection of 777.5 nm emission was subsequently observed in imaging studies of atomic oxygen in flames.<sup>13,14</sup> These observations suggest the occurrence of excitation transfer from the  $3p$  to the  $5p$  state (see Figure 1). The interpretation of these experiments in terms of specific bimolecular rate processes is not straightforward because of the high pressure (1 atmosphere) and chemical complexity of these flames. In addition, at least in the experiment of Miziolek and DeWilde,<sup>5</sup> the tightly focused laser probe was observed to be promoting multiphoton photolysis of the oxidizer as well as the fuel molecules, leading to a two-photon resonant formation of a microplasma. Nevertheless, even under conditions of no apparent laser probe volume perturbation, it appears that spin-changing collisions of the initially excited level could be a significant collisional removal pathway for laser excited oxygen  $3p\ ^3P$  atoms. In order to employ two-photon excitation for quantitative measurements in combustion environments, such as propellant flames, it is necessary to understand the mechanism for transfer of the initial excitation energy.

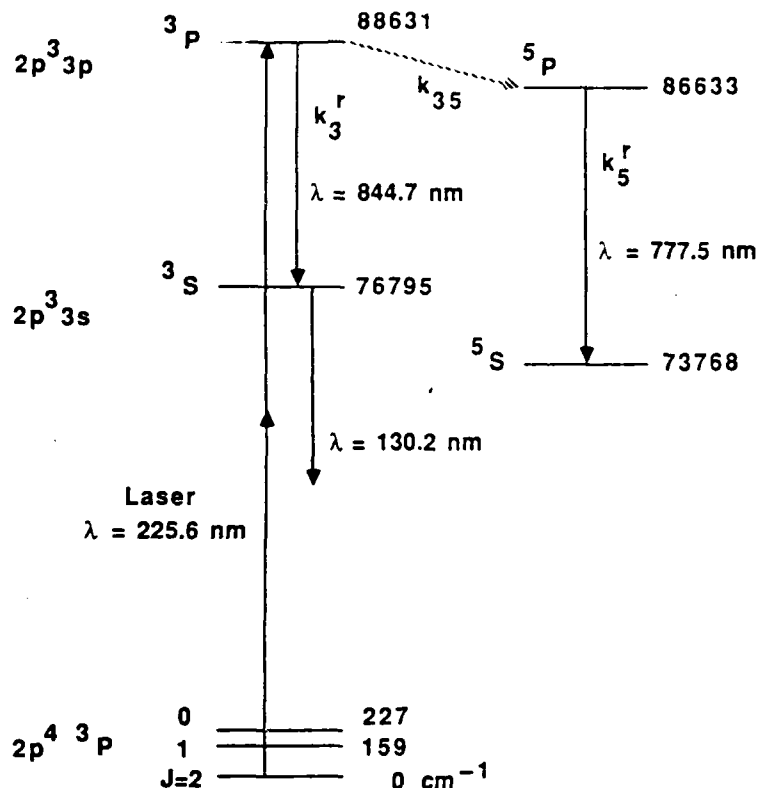


Figure 1. Relevant Energy Levels for Two-Photon Excitation of Oxygen Atoms and Excited-State Collisional Energy Transfer. The electronic energies, taken from Ref. 16 are given in  $\text{cm}^{-1}$ , and allowed radiative transitions are denoted, with wavelengths given in nm. The denoted radiative and collisional rate constants are defined in Section B.

The present experimental study was undertaken to investigate collisional excitation transfer from the oxygen  $3p^3 3p$  to  $5p$  states in a controlled low-pressure environment. Previous studies<sup>1,6,8</sup> of collisional processes involving the  $3p$  state have centered on the measurement of total quenching rate constants with closed-shell collisional partners, such as the inert gases, nitrogen molecules, etc. Simple theoretical considerations<sup>16</sup> suggest that open-shell free radical species will be more effective in inducing spin-changing excitation transfer to the  $5p$  state. Approach of an open-shell perturber species in a state of, say, doublet spin multiplicity to an oxygen atom in the  $3p^3 3p$  state will yield both doublet and quartet molecular curves, while approach to the  $5p$  state yields quartet and sextet states. Crossing of quartet curves originating from the  $3p$  and  $5p$  asymptotes will provide a spin-allowed mechanism for collision-induced transitions between the  $3p$  and  $5p$  states, which is not possible with closed-shell partners. This argument ignores the possible importance of excitations in the collision partner.

In the present study, we compare the propensity of the stable open-shell oxygen molecule and the closed-shell nitrogen molecule to induce  $3p \rightarrow 5p$

transitions. Previous experiments<sup>1,6,8</sup> have determined the total bimolecular quenching rate constants for quenching of the  $^3P$  state by these molecules.

## II. EXPERIMENTAL

The apparatus employed for these experiments is shown in Figure 2. Oxygen atoms were generated by passing a mixture of helium and oxygen (typical partial pressures of 1.2 and 0.2 Torr, respectively) through an Evenson-Broida 2450 MHz resonant cavity. UHP grade gases were obtained from Linde and used without further purification. The walls of discharge tube were coated with phosphoric acid to reduce atomic recombination on the surfaces.<sup>17</sup> The forward microwave power was kept relatively low (<25 W) in order to minimize the fractional dissociation of the oxygen molecules and production of other transient species. Nevertheless, this production scheme prepared sufficient densities of ground-state oxygen atoms for these experiments. The quenching gases, either  $N_2$  or additional  $O_2$ , were added downstream of the microwave discharge. Pressures were measured by a capacitance manometer. The flow tube was pumped by a 50 cfm single-stage mechanical pump.

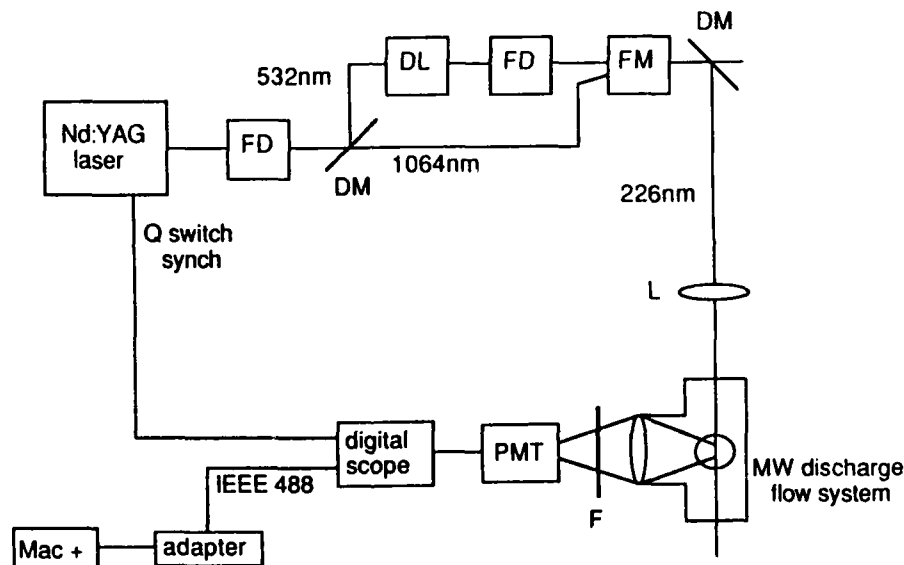


Figure 2. Schematic Diagram of the Experimental Apparatus.  
DL: dye laser; FD: frequency-doubling crystal; FM: frequency-mixing crystal; DM: dichroic mirror; L: lens; F: interference filter; PMT: photomultiplier tube.

The laser excitation and fluorescence detection zone was located 10 cm beyond a 90° bend Wood's horn light trap, which itself was placed just past the microwave discharge. Two-photon excitation of oxygen atoms was accomplished with tunable uv radiation from a Nd:YAG pumped, frequency doubled and mixed dye laser (Quantel) which operated at a 10 Hz repetition rate. The dye solution in the latter was a concentration- and composition-tuned mixture



of rhodamine 590 and 610. The 226 nm radiation was separated from other wavelengths by a dichroic mirror; this separation technique was preferred over the use of prisms since, with the former, the laser beam position through the flow system does not change with wavelength. Typical uv power at the apparatus was approximately 1 mJ per pulse, and the bandwidth of the doubled and mixed radiation was ca. 1 cm<sup>-1</sup> FWHM. The radiation was focused into the center of a flow system with a 30 cm Suprasil lens. No photolytic effects due to laser decomposition of molecular oxygen were evident, as observation of the O atom two-photon signal required the presence of both molecular oxygen and microwave radiation.

The fluorescence was collected at right angles to the laser beam with a fast (f/2) Suprasil lens and focused through a filter onto a red-sensitive photomultiplier tube (EMI 9516QB). The filters employed were a 850 nm center wavelength, 25 nm bandpass interference filter for detection of the <sup>3</sup>P → <sup>3</sup>S emission at 844.7 nm and a 780 nm center wavelength, 10 nm bandpass filter for observation of the <sup>5</sup>P → <sup>5</sup>S at 777.5 nm. The measured transmission of these filters was 56 and 66% at 844.7 and 777.5 nm, respectively.

The output from the photomultiplier was passed to a boxcar integrator (Stanford Research Systems) for measuring excitation spectra or to a digital oscilloscope (Tektronix 2430A) for capturing the temporal profiles of fluorescence waveforms. The boxcar integrator and oscilloscope were triggered with a synchronization pulse from the Nd:YAG laser Q switch. Some details about the specifications of the oscilloscope are relevant. The bandwidth of the analog section of this instrument is 125 MHz; the digital sampling rate is 100 megasamples per sec, or 10 nsec between channels. In our experiments we utilized an interpolation feature for repetitive signals, which allowed digitization on a finer grid to achieve the full bandwidth. The waveform from an individual laser pulse was obtained with the usual 10 nsec spacing; however, successive waveforms were taken with a slightly shifted initial delay, controlled internally by the oscilloscope. To improve the signal-to-noise ratio, waveforms were also acquired using a 256-scan running average. Typical emission lifetimes ranged from 40 to 15 nsec, while the laser excitation pulse length was 7 nsec.

The waveforms acquired by the digital oscilloscope were transferred through an IEEE 488 interface to a microcomputer (Apple Macintosh Plus) for storage, generation of hard-copy plots, and analysis.

### III. RESULTS

#### A. Fluorescence Waveforms:

Figure 3 displays typical fluorescence waveforms for emission at 844.7 and 777.5 nm. The noise in these traces is due to the effect of the interpolating feature of the oscilloscope (see Section B) and the large fluctuations in the fluorescence signal between successive laser shots. Under all pressure conditions investigated, the emission at 844.7 nm from the initially excited <sup>3</sup>P level was much stronger. It should also be noted that the relative detection sensitivity (filter transmission plus photomultiplier sensitivity, the latter taken from manufacturer's specifications) was larger (4:1) for the collision-induced <sup>5</sup>P → <sup>5</sup>S feature.

In addition to the differing intensities for the fluorescent decay of the initially excited  $3P$  and collisionally populated  $5P$  states, the two waveforms in Figure 3 have different temporal profiles. The waveform for the  $3P$  state in Figure 3a is the usual exponential curve expected for the decay of an excited level, while that for the  $5P$  state in Figure 3b builds up to the peak intensity after an induction period. The next section presents in detail the equations governing the time dependence of these emissions and shows how rate constants for the various kinetic processes can be extracted.

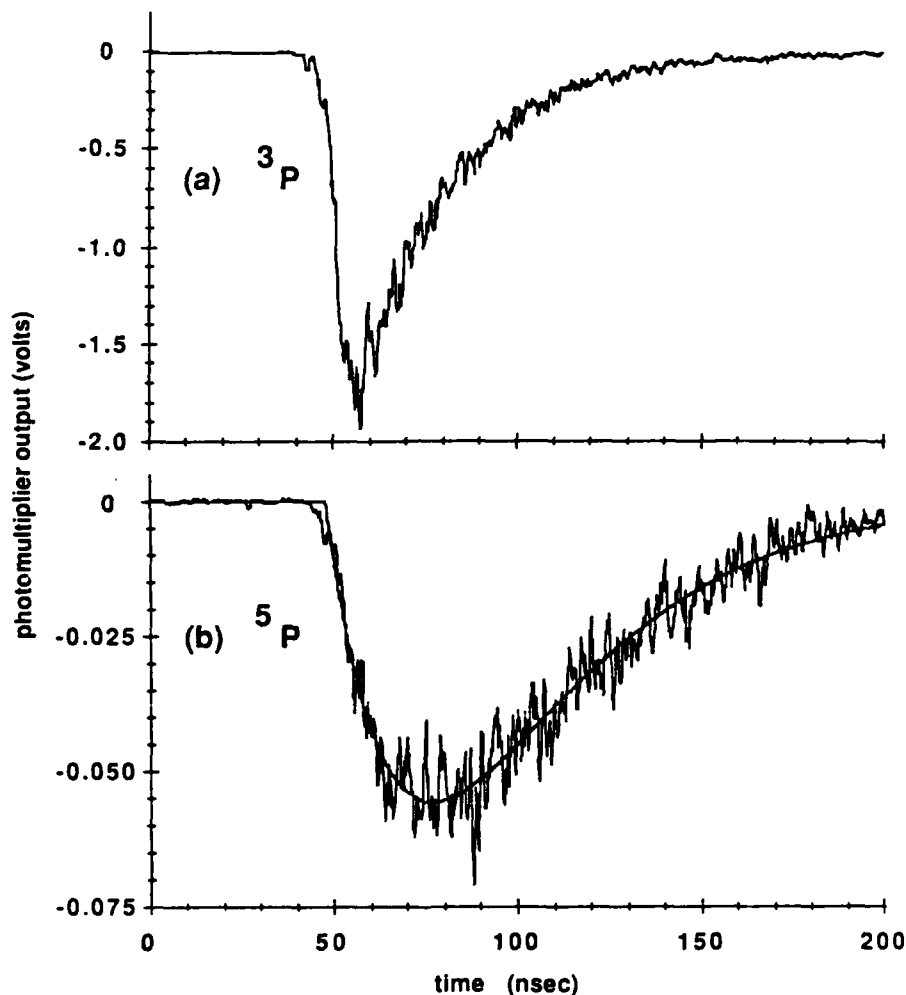


Figure 3. Waveforms for (a) the  $3P \rightarrow 3S$  and (b) the  $5P \rightarrow 5S$  Fluorescence Emission Upon Two-Photon Excitation of the  $3p\ 3P$  State.

Pressures: 1.47 Torr He and 0.30 Torr  $O_2$ . These waveforms were acquired with the same photomultiplier voltage merely by channeling the detection filter.

## B. Kinetic Equations:

The following equations govern the kinetics of decay and energy transfer of the  $3p\ ^3P$  and  $5p\ ^5P$  electronic states of the oxygen atom:

$$dn_3/dt = -n_3k_3, \quad (1)$$

and

$$dn_5/dt = n_3k_{35} - n_5k_5, \quad (2)$$

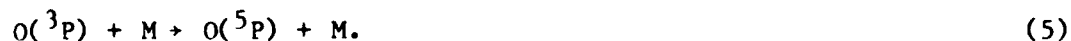
where  $n_3$  and  $n_5$  are the concentrations of the  $^3P$  and  $^5P$  states, respectively, and  $k_3$  and  $k_5$  are the total removal rates by both radiative and collisional processes for the respective atomic states:

$$k_3 = k_3^r + k_3^Q(M)[M] \quad (3)$$

and

$$k_5 = k_5^r + k_5^Q(M)[M]. \quad (4)$$

Here the spontaneous decay rates are denoted by  $k_3^r$  and  $k_5^r$ , while the bimolecular quenching rate constants are indicated as  $k_3^Q(M)$  and  $k_5^Q(M)$ . Equations (3) and (4) are written assuming there is only one quenching species, of concentration  $[M]$ , present. The generalization to several collision partners is obvious. These quenching rate constants represent the total rate of collisional removal of the relevant atomic species. The quantity  $k_{35}$  in Eq. (2) represents that portion of the collisional removal of the  $^3P$  state which results in energy transfer to the  $^5P$  state:



We write

$$k_{35} = k_{35}(M)[M], \quad (6)$$

where  $k_{35}(M)$  is the bimolecular rate constant for process.<sup>5</sup>

We assume that the two-photon laser excitation to the  $^3P$  state yields a concentration  $n_3^{(0)}$  in this state at  $t=0$ . Equations (1) and (2) may be readily integrated. The  $^3P$  state follows a simple exponential decay:

$$n_3 = n_3^{(0)} \exp(-k_3t), \quad (7)$$

while the time dependence of the  $^5P$  state is given by the difference of two exponentials:

$$n_5 = \frac{n_3^{(0)}k_{35}[\exp(-k_5t) - \exp(-k_3t)]}{k_3 - k_5} \quad (8)$$

Thus, we see that the time dependence of the  $^3P$  population follows the usual exponential decay, while that of the  $^5P$  state builds up to a maximum after some delay.

Equation (7) shows that the  $^3P$  radiative lifetime and quenching rate constants may be determined by measurement of the decay lifetime  $\tau = k_3^{-1}$  as a function of quench gas pressure, in the usual Stern-Vollmer treatment. The corresponding quantities for the  $^5P$  state must be determined in a nonlinear least squares treatment of the  $^5P$  concentration as a function of time, according to Eq. (8). The time dependence of the  $^3P$  and  $^5P$  concentrations can be determined from the emission intensities at 844.7 and 777.5 nm, respectively.

The  $^3P + ^5P$  transfer rate  $k_{35}$  cannot be determined from analysis of the fluorescence waveforms alone, but rather from the ratio of the integrated emission intensities. The integrated fluorescence intensity for the decay of the  $^3P$  state is proportional to

$$I_3 = k_3^F \int_0^\infty n_3 dt. \quad (9a)$$

With the help of Eq. (7), this equals

$$I_3 = n_3^{(0)} (k_3^F/k_3). \quad (9b)$$

The quantity in parentheses in Eq. (9b) may be identified with the fluorescence quantum yield for the  $^3P$  state. The integrated emission intensity for the  $^5P$  state is given by

$$I_5 = k_5^F \int_0^\infty n_5 dt, \quad (10a)$$

which, with Eq. (8), becomes

$$I_5 = k_{35} n_3^{(0)} (k_5^F/k_5 k_3). \quad (10b)$$

Thus, the ratio of these integrated emission intensities equals

$$I_5/I_3 = (k_{35}/k_3^F) (k_5^F/k_5). \quad (11)$$

The rightmost quantity in parentheses in Eq. (11) is the  $^5P$  fluorescence quantum yield, while the ratio of  $k_{35}/k_3^F$  represents the ratio of  $^3P + ^5P$  energy transfer collisions to  $^3P$  radiative decay events.

### C. Quenching Rate Constants:

Quenching rate constants for the  $^3P$  state were determined from linear least squares fits of the logarithm of the  $^3P + ^3S$  emission as a function of time from fluorescence decay curves, similar to that presented in Figure 3a, at different quencher concentrations. A Stern-Vollmer plot for  $O_2$  is presented in Figure 4a. In this figure, the abscissa is the total  $O_2$  partial pressure including oxygen passing through the microwave discharge and added downstream. For measurement of both  $O_2$  and  $N_2$  quenching rate constants, helium and oxygen, at typical pressures of approximately 1.3 and 0.2 Torr, respectively, were passed through the discharge. Using the previously measured<sup>6</sup> quenching rate constant for helium, we calculate that collisional removal by this species is small under our conditions, approximately  $0.07 \times 10^7 \text{ s}^{-1}$ . In principle, the transient free radical species generated by the discharge could also contribute to collisional quenching. However, we found

that the decay rate  $k_3$  was the same with low (20 W) or high (50 W) microwave power applied to the cavity.

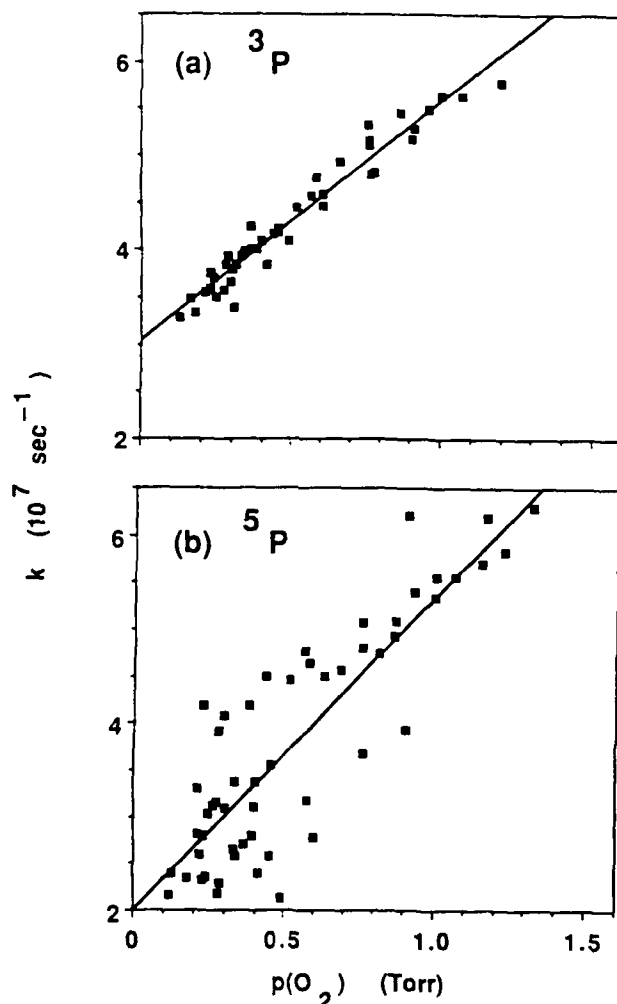


Figure 4. Stern-Volmer Plots for (a) the  $^3P \rightarrow ^3S$  Emission at 844.7 nm and (b) the  $^5P \rightarrow ^5S$  Emission at 777.5 nm as a Function of  $O_2$  Quencher Partial Pressure

Linear least squares fits (the solid line in Figure 4a) of these data yields the following bimolecular rate constants listed in Table 1 for the total collisional removal rate of the  $^3P$  state. The intercept for the  $O_2$  plot yields a decay rate of  $(3.05 \pm 0.15) \times 10^7 \text{ s}^{-1}$ . Correcting for the expected contribution due to helium quenching (see above), we obtain the radiative decay rate for the  $^3P$  state:  $k_3^r = (2.98 \pm 0.15) \times 10^7 \text{ s}^{-1}$ . This corresponds to an estimated  $^3P$  radiative lifetime of  $33.3 \pm 1.7 \text{ nsec}$ . The quoted uncertainties for all rate constants represent 3 standard deviations.

Table 1. Bimolecular Rate Constants for Quenching and Collisional Transfer of the  $3p\ ^3P$  and  $5p$  States of the Oxygen Atom at Room Temperature

| Collision Partner | Rate constant<br>(molecule <sup>-1</sup> cm <sup>3</sup> s <sup>-1</sup> ) | This Study                      | Previous Determinations  |
|-------------------|--|---------------------------------|--|
| O <sub>2</sub>    | k <sub>3</sub> <sup>0</sup>  | (7.8±0.8) X 10 <sup>-10</sup>   | (8.64±0.16) X 10 <sup>-10</sup> Ref. 8<br>(6.3±0.12) X 10 <sup>-10</sup> Ref. 6b |
|                   | k <sub>5</sub> <sup>0</sup>  | (10.8±1.8) X 10 <sup>-10</sup>  |  |
|                   | k <sub>35</sub>  | 6 X 10 <sup>-11</sup> *         |  |
| N <sub>2</sub>    | k <sub>3</sub> <sup>0</sup>  | (5.87±0.15) X 10 <sup>-10</sup> | (4.3±0.74) X 10 <sup>-10</sup> Ref. 6b<br>(2.5±0.1) X 10 <sup>-10</sup> Ref. 1   |
|                   | k <sub>35</sub>  | 2 X 10 <sup>-11</sup> *         |  |

\*Estimated experimental uncertainty of a factor of 2.

The collisional and radiative decay rate for the  $5p$  state was obtained from analysis of  $5p \rightarrow 5s$  decay curves such as that presented in Figure 3b. Because of the weakness of the  $5p \rightarrow 5s$  emission signals, this analysis was carried out only for O<sub>2</sub> quencher. The total decay rate k<sub>5</sub> was determined by nonlinear least squares fits<sup>18</sup> using the expected functional form in Eq. (8) for the time dependence of the  $5p$  population. In this fit, the decay rate k<sub>3</sub> for the  $3p$  state was fixed at the value calculated from the Stern-Vollmer plot in Figure 4a for the O<sub>2</sub> partial pressure in the given scan. Parameters allowed to vary in this nonlinear fit were the decay rate k<sub>5</sub>, an overall normalization constant (proportional to k<sub>35</sub>), and the channel for which t=0. The solid line in Figure 3b represents the fit to the experimental data given in that plot.

The derived decay rates k<sub>5</sub> from nonlinear least squares analysis of  $5p \rightarrow 5s$  emission waveforms are presented in Figure 4b. It can be seen that the scatter of the calculated rate constants is large. This is due mainly to the smallness of these emission signals, which arise not directly from the initially populated state but rather by collisional transfer. A Stern-Vollmer analysis of these rate constants was performed (solid line in Figure 4b) and yield the following estimates for the bimolecular quenching rate constant by O<sub>2</sub> and the radiative decay rate: k<sub>5</sub><sup>0</sup>(O<sub>2</sub>) = (10.8±1.8) X 10<sup>-10</sup> molecule<sup>-1</sup> cm<sup>3</sup> s<sup>-1</sup> (included in Table 1) and k<sub>5</sub><sup>r</sup> = (2.01±0.35) X 10<sup>7</sup> s<sup>-1</sup>. This corresponds to an estimated radiative lifetime of 50±9 nsec.

#### D. Energy Transfer Rate Constants:

Equation (11) shows that measurement of the ratio of the integrated emission intensities for  $5p \rightarrow 5s$  and  $3p \rightarrow 3s$  fluorescence decay can yield the rate constant k<sub>35</sub> for collisional transfer from the  $3p$  to the  $5p$  state. Accordingly, a series of experiments were carried out to record these waveforms under identical pressure conditions. For a given partial pressure

of added quench gas, the fluorescence waveform for one of these radiative decay paths was recorded; then the filter was switched and the other recorded immediately thereafter. The integrated signals were calculated and their ratios corrected for the relative detection sensitivity at 844.7 and 777.5 nm.

Figure 5 displays the derived integrated  $5p \rightarrow 5s$  to  $3p \rightarrow 3s$  intensity ratios, corrected for the wavelength response of the photomultiplier, as a function of both added  $O_2$  and added  $N_2$  gas. The scatter in these data is again large, reflecting the large fluctuations in the fluorescence signal from laser shot to shot. Nevertheless, it can be seen that for both collision partners this ratio is always small and never increases beyond 5%.

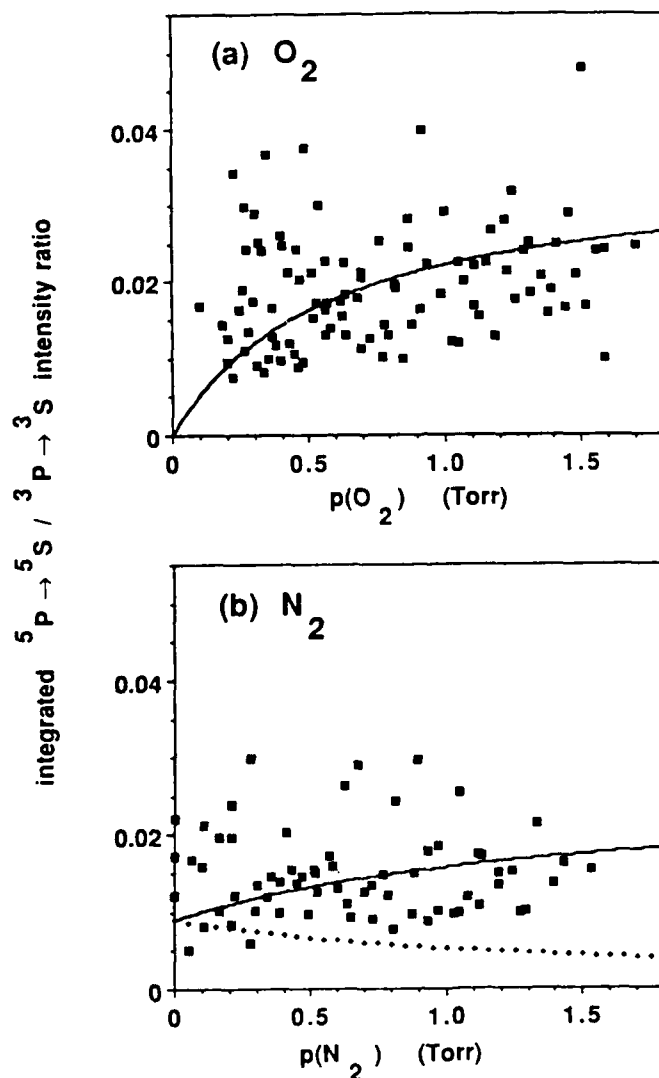


Figure 5. Ratio of the Integrated  $5p \rightarrow 5s$  to  $3p \rightarrow 3s$  Emission Intensity (Corrected for the Wavelength Sensitivity of the Photomultiplier) Versus Added (a)  $O_2$  and (b)  $N_2$ . The solid curves represent the best fits to the intensity ratio versus quench gas pressure. The dotted curve in (b) shows the expected intensity ratio if  $k_{35}(N_2)$  were equal to zero.

In spite of the large experimental uncertainties in the integrated intensity ratio, we may still obtain estimates of the rate constants for  $^3\text{P} \rightarrow ^5\text{P}$  collisional transfer. For the case of  $\text{O}_2$ , for which the data are displayed in Figure 5a, the integrated intensity ratio can be expressed as a function of the  $\text{O}_2$  density  $n(\text{O}_2)$  as

$$\frac{I_5}{I_3} = \frac{A n(\text{O}_2)}{1 + n(\text{O}_2)/n_0} \quad (12)$$

where

$$A = k_{35}(\text{O}_2)/k_3^r, \quad (13)$$

and

$$n_0 = k_5^r/k_5^0(\text{O}_2). \quad (14)$$

The quantity  $n_0$  can be calculated from the Stern-Vollmer analysis (Figure 4(b)) for the  $^5\text{P}$  state and equals  $1.9 \times 10^{16}$  molecules  $\text{cm}^{-3}$  (or 0.58 Torr).

Thus, Eq. (12) can be fit to the data in Figure 5a by a linear least squares fit<sup>18</sup> to determine the coefficient A in Eq. (12). Using our derived value for the  $^3\text{P}$  radiative decay rate  $k_3^r$ , we find that the rate constant  $k_{35}(\text{O}_2)$  equals  $6 \times 10^{-11}$  molecule $^{-1}$   $\text{cm}^3 \text{s}^{-1}$ . We estimate an uncertainty of approximately a factor of 2 in this value, due to the scatter in the determined intensity ratios given in Figure 5 and the uncertainty in the relative detection sensitivity. The contribution to the uncertainty in  $k_{35}(\text{O}_2)$  due to possible error in  $k_3^r$  is less than that from the scatter in the measured intensity ratios. The solid curve in Figure 5a represents the best fit to the integrated intensity ratio as a function of added  $\text{O}_2$ .

Because of the presence of a small amount of  $\text{O}_2$  to generate oxygen atoms, the dependence of the integrated intensity ratio on added  $\text{N}_2$  density  $n(\text{N}_2)$  differs somewhat from Eq. (12). In this case, we have

$$\frac{I_5}{I_3} = \frac{B}{C + n(\text{N}_2)/n_N} + \frac{Dn(\text{N}_2)}{C + n(\text{N}_2)/n_N} \quad (15)$$

where

$$B = k_{35}(\text{O}_2) n(\text{O}_2)/k_3^r, \quad (16)$$

$$C = 1 + n(\text{O}_2)/n_0, \quad (17)$$

$$D = k_{35}(\text{N}_2)/k_3^r, \quad (18)$$

and

$$n_N = k_5^r/k_5^0(\text{N}_2). \quad (19)$$



The parameters B and C are known from the analysis of the  $O_2$  data. We have not studied the quenching of the  $^5P$  state by  $N_2$ . In view of the similarity of the  $^3P$  and  $^5P$  quenching rate constants by  $O_2$ , within the large experimental uncertainties particularly of the latter, we assume that  $k_{35}^O(N_2)$  in Eq. (19) equals the corresponding rate constant for the  $^3P$  state. We thus calculate  $n_N$  to equal  $3.4 \times 10^{16}$  molecules  $cm^{-3}$  (or 1.05 Torr).

The transfer rate constant  $k_{35}(N_2)$  may be calculated by a linear least squares fit, similar to that used for the corresponding rate constant for  $O_2$ , to determine the parameter D in Eq. (15). We find that  $k_{35}(N_2)$  equals  $2 \times 10^{-11}$  molecule $^{-1}$   $cm^3$  s $^{-1}$ , with an estimated factor of 2 uncertainty. The solid curve in Figure 5b represents the best fit to the integrated intensity ratio as a function of added  $N_2$ . This value for  $k_{35}(N_2)$  depends on assuming that the  $^3P$  and  $^5P$  quenching rate constants for  $N_2$  are the same. If the  $^5P$  rate were only half as large, then the derived value for  $k_{35}(N_2)$  would be reduced by ca. 30%, which is within the estimated experimental uncertainties. To show that  $^3P \rightarrow ^5P$  collisional transfer is significant with  $N_2$  collision partner, we have also plotted with a dotted curve in Figure 5b the expected integrated intensity ratio if  $k_{35}(N_2)$  were equal to zero. The rate constants  $k_{35}$  for both  $O_2$  and  $N_2$  are also included in Table 1.

#### IV. DISCUSSION

Table 1 compares our quoted  $3p\ ^3P$  total quenching rate constants with those determined in previous studies. Our value for  $O_2$  agrees well with that of Bamford, et al.,<sup>8</sup> and is somewhat higher than the most recent result<sup>6b</sup> from Kohse-Hoinghaus and coworkers. The present result for the corresponding rate constant for quenching by  $N_2$  is also slightly higher than that of Kohse-Hoinghaus and coworkers.<sup>6b</sup> By contrast, the earliest measurement of the  $N_2$  quenching rate constant by Bischel, et al.,<sup>1</sup> is considerably smaller than the present result and that of Ref. 6b. We do not know the reason for this discrepancy.

The present result for the  $3p\ ^3P$  radiative lifetime ( $33.6 \pm 1.7$  nsec), derived from the intercept of the Stern-Vollmer plot for  $^3P$  quenching by  $O_2$  (Figure 4a), agrees reasonably well with previous determinations of this lifetime. By similar observation of time-resolved two-photon laser-induced fluorescence, Bamford, et al.,<sup>8</sup> Bittner, et al.,<sup>6b</sup> and Kroll, et al.,<sup>19</sup> obtain values of  $34.7 \pm 3.7$ ,  $36.2 \pm 0.69$ , and  $36 \pm 4$  nsec, respectively. The measurement of Bischel, et al.,<sup>1</sup> who also monitored the emission after two-photon laser excitation and report  $\tau(3p\ ^3P) = 39.1 \pm 1.4$  nsec, and that of Bromander, et al.,<sup>20</sup> who employed a high frequency electron beam deflection technique and find  $\tau(3p\ ^3P) = 40 \pm 3$  nsec, yield lifetimes somewhat longer than the more recent experimental results. There have been several earlier determinations, involving absolute emission intensity measurements, of the  $3p\ ^3P \rightarrow 3s\ ^3S$  radiative decay rate, and hence  $3p\ ^3P$  radiative lifetime, since the upper state has only one electric-dipole-allowed decay pathway. The compilation of Wiese, et al.,<sup>21</sup> gives a value of  $\tau(3p\ ^3P) = 35.7$  nsec. The theoretical calculations of Pradhan and Saraph<sup>22</sup> yields a somewhat smaller result:  $\tau(3p\ ^3P) = 30.3$  nsec. The former is in reasonable agreement with recent time-resolved experiments, while the latter appears to be slightly small.

Our experimental determination of the  $3p\ ^5P$  radiative lifetime,  $\tau(3p\ ^5P) = 50 \pm 9$  nsec, appears to be somewhat longer than previous estimates of this

quantity. The present measurement suffers from difficulties in extracting the  $^5P$  decay rate  $k_5$  in a nonlinear least squares fit to  $^5P \rightarrow ^5S$  emission waveforms with low signal to noise ratio such as that displayed in Figure 3b. There has been only one other time-resolved determination of the  $3p\ ^5P$  radiative lifetime. Using the high-frequency electron beam deflection technique, Bromander, et al.,<sup>20</sup> report  $\tau(3p\ ^5P) = 39 \pm 2$  nsec. The compilation of Wiese, et al.,<sup>21</sup> yields a value of 29 nsec, while a result of 28 nsec is obtained from the calculations of Pradhan and Saraph.<sup>22</sup> The oscillator strengths computed by Pradhan and Saraph<sup>22</sup> have recently been shown by comparison with electron scattering results to be reliable to better than 20%, at least for transitions out of the ground  $2p^4\ ^3P$  state.<sup>23</sup>

To our knowledge, there have been no previous experimental determinations of collisional properties of the  $3p\ ^5P$  state. While the exact value for the  $^5P$  quenching rate constant by  $O_2$  may be uncertain because of difficulties such as those discussed in the previous paragraph, the present experiment nevertheless indicates that this quenching is large and comparable to that for the neighboring  $^3P$  state. In attempting to understand the variation of the rate constants for quenching of the nitrogen atom  $3p\ ^4D$  state by the inert gases, Copeland, et al.,<sup>7</sup> noted the importance of the availability of excited states in both the excited atom and the quencher to understand the mechanism of quenching. For the oxygen atom, it is interesting that the overall quenching rate for the  $3p\ ^3P$  and  $^5P$  states by  $O_2$  are both large, despite the fact that the former can be removed by excitation transfer to the  $^5P$  state, which lies only ca.  $2000\text{ cm}^{-1}$  lower, while excitation transfer to lower  $O$  atom  $3s$  states for the latter would require removal of ca.  $12000\text{ cm}^{-1}$  (see Figure 1). This suggests that excited states of the  $O_2$  collision partner may be of importance.

The ratio of the rate constants  $k_{35}(M)$  to  $k_3^0(M)$  equals the fraction  $f_T$  of  $^3P$  quenching collisions which result in excitation transfer to the lower-lying  $^5P$  state. Despite the factor of 2 uncertainty in our measured excitation transfer rate constants, it is nevertheless clear that  $^3P \rightarrow ^5P$  collisional transfer explains only a small fraction of the  $^3P$  quenching. For  $O_2$  and  $N_2$ , we find that  $f_T$  equals approximately 8% and 3%, respectively. While  $f_T$  is significantly lower for the closed-shell  $N_2$  molecule than for  $O_2$ , nevertheless this excitation transfer process is not insignificant for the former. This suggests that the model for this process given in the Introduction may be too simplistic.

We surmise that the bulk of  $^3P$  quenching collisions occurs by excitation transfer to the collision partner, rather than collision-induced transitions to lower-lying oxygen atom states. This intermolecular excitation transfer would be expected to populate quencher electronic states whose energies lie close to that of the incident  $^3P$  state. The initial internal energy of the former is quite high, ca.  $88600\text{ cm}^{-1}$  (see Figure 1), and both  $O_2$  and  $N_2$  possess a number of potential acceptor excited electronic states in this energy range.<sup>24</sup> As the initial excitation energy is greater than the  $O_2$  and  $N_2$  bond energies, dissociative excitation transfer can also occur.

The participation of excited acceptor states in the collisional decay of the  $^3P$  state would explain why the model for  $^3P \rightarrow ^5P$  collision-induced transitions given in the Introduction is inadequate. Verification of the importance of intermolecular excitation transfer in the quenching of the  $3p\ ^3P$

state could be obtained by observation of excited molecular emission, in the same way that we have shown the existence of intramolecular  $3p \rightarrow 5p$  collisional transitions. For example, in the case of  $N_2$  the well-known  $C^3\Pi_u$  state has excitation energy very close to that of the O atom  $3p$  state; this electronic state emits in the second positive system in the ultraviolet.<sup>24</sup> Quenching of the  $3p$  state by  $N_2$  can also proceed by a chemical path, namely  $O(3p\ ^3P) + N_2 \rightarrow NO + N$ .

The large uncertainties in the rate constants  $k_{35}(M)$  result from the large scatter in the measured integrated intensity ratios  $I_5/I_3$  (see Figure 5). These fluctuations would be considerably reduced if the integrated signals  $I_5$  and  $I_3$  were measured simultaneously with two photomultiplier detectors, rather than sequentially as in the present experiment. In this way, the intensity ratio would be corrected for shot-to-shot fluctuations in the laser pulse energy and spectral profile. Unfortunately, modification of the apparatus to allow dual photomultiplier detection was not possible in this experimental study.

#### ACKNOWLEDGEMENT

We are indebted to Dr. Chen Hsu, of CRDEC at Edgewood, MD, for the loan of a frequency mixing crystal while our crystal was being repolished. BEF and AWM acknowledge partial support from the Air Force Office of Scientific Research, Directorate of Aerospace Sciences, Contract Number 88-0013. The work at Johns Hopkins University was supported in part by the National Science Foundation and the U.S. Army Research Office.

## REFERENCES

1. W.K. Bischel, B.E. Perry, and D.R. Crosley, "Two-Photon Laser Induced Fluorescence in Oxygen and Nitrogen Atoms," Chem. Phys. Lett., Vol. 82, p. 85, 1981; "Detection of Fluorescence from O and N Atoms Induced by Two-Photon Absorption," Appl. Opt., Vol. 21, p. 1419, 1982.
2. R.P. Lucht, J.T. Salmon, G.B. King, D.W. Sweeney, and N.M. Laurendeau, "Two-Photon-Excited Fluorescence Measurement of Hydrogen Atoms in Flames," Opt. Lett., Vol. 8, p. 365, 1983.
3. M. Alden, H. Edner, P. Grafstrom, and S. Svanberg, "Two-Photon Excitation of Atomic Oxygen in a Flame," Opt. Commun., Vol. 42, p. 244, 1982.
4. M. Alden, A.L. Schawlow, S. Svanberg, W. Wendt, and P.L. Zhang, "Three-Photon-Excited Fluorescence Detection of Atomic Hydrogen in an Atmospheric Pressure Flame," Opt. Lett., Vol. 9, p. 211, 1984.
5. A.W. Miziolek and M.A. DeWilde, "Multiphoton Photochemical and Collisional Effects During Oxygen-Atom Flame Detection," Opt. Lett., Vol. 9, p. 390, 1984.
6. (a) U. Meier, K. Kohse-Hoinghaus, and Th. Just, "H and O Atom Detection for Combustion Applications: Study of Quenching and Laser Photolysis Effects," Chem. Phys. Lett., Vol. 126, p. 567, 1986; (b) J. Bittner, K. Kohse-Hoinghaus, U. Meier, and Th. Just, "Quenching of Two-Photon Excited H ( $3s, 3d$ ) and O ( $3p\ ^3P_{1,2,0}$ ) Atoms by Rare Gases and Small Molecules," Chem. Phys. Lett., Vol. 143, p. 571, 1988.
7. R.A. Copeland, J.B. Jeffries, A.P. Hickman, and D.R. Crosley, "Radiative Lifetime and Quenching of the  $3p\ ^4D^0$  State of Atomic Nitrogen," J. Chem. Phys., Vol. 86, p. 4876, 1987.
8. D.J. Bamford, L.E. Jusinski, and W.K. Bischel, "Absolute Two-Photon Absorption and Three Photon Ionization Cross Sections for Atomic Oxygen Atoms," Phys. Rev. A, Vol. 34, p. 185, 1986.
9. J.E.M. Goldsmith, "Resonant Multiphoton Optogalvanic Detection of Atomic Hydrogen in Flames," Opt. Lett., Vol. 7, p. 437, 1982; "Resonant Multiphoton Optogalvanic Detection of Oxygen Atoms in Flames," J. Chem. Phys., Vol. 78, p. 1610, 1983.
10. J.E.M. Goldsmith, "Flame Studies of Atomic Hydrogen and Oxygen Using Resonant Multiphoton Optogalvanic Spectroscopy," 20th Symposium (International) on Combustion, The Combustion Institute, Pittsburgh, p. 13, 1984.
11. J.E.M. Goldsmith, "Photochemical Effects in Two-Photon Excited Fluorescence Detection of Atomic Oxygen in Flames," Appl. Optics, Vol. 26, p. 3566, 1987.
12. P.J.H. Tjossem and T.A. Cool, "Detection of Atomic Hydrogen in Flames by Resonance Two-Photon Ionization at 365 nm," Chem. Phys. Lett., Vol. 100, p. 479, 1983.

13. M. Alden, H.M. Hertz, S. Svanberg, and S. Wallin, "Imaging Laser-Induced Fluorescence of Oxygen Atoms in a Flame," Appl. Opt., Vol. 23, p. 325, 1984.
14. J.E.M. Goldsmith and R.J.M. Anderson, "Imaging of Atomic Hydrogen in Flames with Two-Step Saturated Fluorescence Detection," Appl. Opt., Vol. 24, p. 607, 1985.
15. C.E. Moore, Atomic Energy Levels, Vol. 1, NSRDS-NBS 35, US Government Printing Office, Washington, 1971.
16. M.H. Alexander, private communication.
17. D.W. Setser, ed., Reactive Intermediates in the Gas Phase, Academic, New York, 1979.
18. P.R. Bevington, Data Reduction and Error Analysis for the Physical Sciences, McGraw-Hill, New York, 1969.
19. S. Kroll, H. Lundberg, A. Persson, and S. Svanberg, "Time-Resolved Laser Spectroscopy of High-Lying States in Neutral Oxygen," Phys. Rev. Lett., Vol. 55, p. 284, 1985.
20. J. Bromander, N. Duric, P. Erman, and M. Larsson, "Lifetimes of Some Levels in Neutral Carbon, Nitrogen, and Oxygen," Phys. Scr., Vol. 17, p. 119, 1978.
21. W.L. Wiese, M.W. Smith, and B.M. Glennon, Atomic Transition Probabilities, Vol. 1, NSRDS-NBS 4, US Government Printing Office, Washington, 1966.
22. A.K. Pradhan and H.E. Saraph, "Oscillator Strengths for Dipole Transitions in Neutral Oxygen," J. Phys. B, Vol. 10, p. 3365, 1977.
23. J.P. Doering, E.E. Gulcicek, and S.O. Vaughan, "Electron Impact Measurement of Oscillator Strengths for Dipole-Allowed Transitions of Atomic Oxygen," J. Geophys. Res., Vol. 90, p. 5279, 1985.
24. K.P. Huber and G. Herzberg, Molecular Spectra and Molecular Structure. IV. Constants of Diatomic Molecules, Van Nostrand Reinhold, New York, 1979.

# DISTRIBUTION LIST

| <u>No. Of</u><br><u>Copies</u> | <u>Organization</u>   | <u>No. Of</u><br><u>Copies</u> | <u>Organization</u>  |
|--------------------------------|---|--------------------------------|--|
| 12                             | Administrator<br>Defense Technical Info Center<br>ATTN: DTIC-DDA<br>Cameron Station<br>Alexandria, VA 22304-6145                  | 1                              | Commander<br>US Army Aviation Systems<br>Command<br>ATTN: AMSAV-DACL<br>4300 Goodfellow Blvd.<br>St. Louis, MO 63120-1798  |
| 1                              | HQ DA (SARD-TR)<br>Washington, DC 20310-0001  | 1                              | Director<br>US Army Aviation Research<br>and Technology Activity<br>Ames Research Center<br>Moffett Field, CA 94035-1099   |
| 1                              | Commander<br>US Army Materiel Command<br>ATTN: AMCDRA-ST<br>5001 Eisenhower Avenue<br>Alexandria, VA 22333-0001                   | 4                              | Commander<br>US Army Research Office<br>ATTN: R. Ghirardelli<br>D. Mann<br>R. Singleton<br>R. Shaw<br>P.O. Box 12211<br>Research Triangle Park, NC<br>27709-2211 |
| 1                              | Commander<br>US Army Laboratory Command<br>ATTN: AMSLC-DL<br>Adelphi, MD 20783-1145   |                                |  |
| 1                              | Commander<br>Armament RD&E Center<br>US Army AMCCOM<br>ATTN: SMCAR-MSI<br>Picatinny Arsenal, NJ 07806-5000                        |                                |  |
| 1                              | Commander<br>Armament RD&E Center<br>US Army AMCCOM<br>ATTN: SMCAR-TDC<br>Picatinny Arsenal, NJ 07806-5000                        | 2                              | Commander<br>Armament R&D Center<br>US Army AMCCOM<br>ATTN: SMCAR-LCA-G,<br>D.S. Downs<br>J.A. Lannon<br>Dover, NJ 07801   |
| 1                              | Director<br>Benet Weapons Laboratory<br>Armament RD&E Center<br>US Army AMCCOM<br>ATTN: SMCAR-LCB-TL<br>Watervliet, NY 12189-4050 | 1                              | Commander<br>Armament R&D Center<br>US Army AMCCOM<br>ATTN: SMCAR-LC-G,<br>L. Harris<br>Dover, NJ 07801  |
| 1                              | Commander<br>US Army Armament, Munitions<br>and Chemical Command<br>ATTN: SMCAR-ESP-L<br>Rock Island, IL 61299-5000               |                                |  |

# DISTRIBUTION LIST

| <u>No. Of<br/>Copies</u> | <u>Organization</u>  | <u>No. Of<br/>Copies</u> | <u>Organization</u>   |
|--------------------------|--|--------------------------|---|
| 1                        | Commander<br>Armament R&D Center<br>US Army AMCCOM<br>ATTN: SMCAR-SCA-T,<br>L. Stiefel<br>Dover, NJ 07801                        | 1                        | Commander<br>Naval Air Systems Command<br>ATTN: J. Ramnarace,<br>AIR-54111C<br>Washington, DC 20360   |
| 1                        | Commander<br>US Army Missile Command<br>ATTN: AMSMI-AS<br>Redstone Arsenal, AL 35898-5000  | 1                        | Commander<br>Naval Surface Weapons Center<br>ATTN: J.L. East, Jr., G-23<br>Dahlgren, VA 22448-5000  |
| 2                        | Commander<br>US Army Missile Command<br>ATTN: AMSMI-RK, D.J. Ifshin<br>W. Wharton<br>Redstone Arsenal, AL 35898                  | 2                        | Commander<br>Naval Surface Weapons Center<br>ATTN: R. Bernecker, R-13<br>G.B. Wilmot, R-16<br>Silver Spring, MD 20902-5000                      |
| 1                        | Commander<br>US Army Missile Command<br>ATTN: AMSMI-RKA, A.R. Maykut<br>Redstone Arsenal, AL 35898-5249                          | 5                        | Commander<br>Naval Research Laboratory<br>ATTN: M.C. Lin<br>J. McDonald<br>E. Oran<br>J. Shnur<br>R.J. Doyle, Code 6110<br>Washington, DC 20375 |
| 1                        | Commander<br>US Army Tank Automotive Cmd<br>ATTN: AMSTA-TSL<br>Warren, MI 48397-5000   | 1                        | Commanding Officer<br>Naval Underwater Systems<br>Center Weapons Dept.<br>ATTN: R.S. Lazar/Code 36301<br>Newport, RI 02840                      |
| 1                        | Director<br>US Army TRADOC Analysis Cmd<br>ATTN: ATAA-SL<br>White Sands Missile Range,<br>NM 88002-5502                          | 1                        | Superintendent<br>Naval Postgraduate School<br>Dept. of Aeronautics<br>ATTN: D.W. Netzer<br>Monterey, CA 93940                                  |
| 1                        | Commandant<br>US Army Infantry School<br>ATTN: ATSH-CD-CSO-OR<br>Fort Benning, GA 31905-5660                                     | 4                        | AFRPL/DY, Stop 24<br>ATTN: R. Corley<br>R. Geisler<br>J. Levine<br>D. Weaver<br>Edwards AFB, CA 93523-5000                                      |
| 1                        | Office of Naval Research<br>Department of the Navy<br>ATTN: R.S. Miller, Code 432<br>800 N. Quincy Street<br>Arlington, VA 22217 | 1                        | AFRPL/MKPB, Stop 24<br>ATTN: B. Goshgarian<br>Edwards AFB, CA 93523-5000  |



# DISTRIBUTION LIST

| <u>No. Of<br/>Copies</u> | <u>Organization</u>   | <u>No. Of<br/>Copies</u> | <u>Organization</u>   |
|--------------------------|---|--------------------------|---|
| 1                        | AFOSR<br>ATTN: J.M. Tishkoff<br>Bolling Air Force Base<br>Washington, DC 20332  | 1                        | Atlantic Research Corp.<br>ATTN: M.K. King<br>5390 Cherokee Avenue<br>Alexandria, VA 22314  |
| 1                        | AFWL/SIIL<br>Kirtland AFB, NM 87117-5800  | 1                        | Atlantic Research Corp.<br>ATTN: R.H.W. Waesche<br>7511 Wellington Road<br>Gainesville, VA 22065  |
| 1                        | Air Force Armament Laboratory<br>ATTN: AFATL/DLODL<br>Eglin AFB, FL 32542-5000  | 1                        | AVCO Everett Rsch. Lab. Div.<br>ATTN: D. Stickler<br>2385 Revere Beach Parkway<br>Everett, MA 02149   |
| 1                        | NASA<br>Langley Research Center<br>Langley Station<br>ATTN: G.B. Northam/MS 168<br>Hampton, VA 23365  | 1                        | Battelle Memorial Institute<br>Tactical Technology Center<br>ATTN: J. Huggins<br>505 King Avenue<br>Columbus, OH 43201                                      |
| 4                        | National Bureau of Standards<br>ATTN: J. Hastie<br>M. Jacox<br>T. Kashiwagi<br>H. Semerjian<br>US Department of Commerce<br>Washington, DC 20234            | 1                        | Cohen Professional Services<br>ATTN: N.S. Cohen<br>141 Channing Street<br>Redlands, CA 92373  |
| 1                        | OSD/SDIO/UST<br>ATTN: L.H. Caveny<br>Pentagon<br>Washington, DC 20301-7100  | 1                        | Exxon Research & Eng. Co.<br>ATTN: A. Dean<br>Route 22E<br>Annandale, NJ 08801  |
| 1                        | Aerojet Solid Propulsion Co.<br>ATTN: P. Micheli<br>Sacramento, CA 95813  | 1                        | Ford Aerospace and<br>Communications Corp.<br>DIVAD Division<br>Div. Hq., Irvine<br>ATTN: D. Williams<br>Main Street & Ford Road<br>Newport Beach, CA 92663 |
| 1                        | Applied Combustion<br>Technology, Inc.<br>ATTN: A.M. Varney<br>P.O. Box 17885<br>Orlando, FL 32860  | 1                        | General Applied Science<br>Laboratories, Inc.<br>77 Raynor Avenue<br>Ronkonkama, NY 11779-6649  |
| 2                        | Applied Mechanics Reviews<br>The American Society of<br>Mechanical Engineers<br>ATTN: R.E. White<br>A.B. Wenzel<br>345 E. 47th Street<br>New York, NY 10017 | 1                        | General Electric Armament<br>& Electrical Systems<br>ATTN: M.J. Bulman<br>Lakeside Avenue<br>Burlington, VT 05401   |

# DISTRIBUTION LIST

| <u>No. Of<br/>Copies</u> | <u>Organization</u>   | <u>No. Of<br/>Copies</u> | <u>Organization</u>  |
|--------------------------|---|--------------------------|--|
| 1                        | General Electric Company<br>2352 Jade Lane<br>Schenectady, NY 12309   | 2                        | Director<br>Lawrence Livermore<br>National Laboratory<br>ATTN: C. Westbrook<br>M. Costantino<br>P.O. Box 808<br>Livermore, CA 94550              |
| 1                        | General Electric Ordnance<br>Systems<br>ATTN: J. Mandzy<br>100 Plastics Avenue<br>Pittsfield, MA 01203                                  | 1                        | Lockheed Missiles & Space Co.<br>ATTN: George Lo<br>3251 Hanover Street<br>Dept. 52-35/B204/2<br>Palo Alto, CA 94304                             |
| 2                        | General Motors Rsch Labs<br>Physics Department<br>ATTN: T. Sloan<br>R. Teets<br>Warren, MI 48090  | 1                        | Los Alamos National Lab<br>ATTN: B. Nichols<br>T7, MS-B284<br>P.O. Box 1663<br>Los Alamos, NM 87545  |
| 2                        | Hercules, Inc.<br>Allegany Ballistics Lab.<br>ATTN: R.R. Miller<br>E.A. Yount<br>P.O. Box 210<br>Cumberland, MD 21501                   | 1                        | National Science Foundation<br>ATTN: A.B. Harvey<br>Washington, DC 20550   |
| 1                        | Honeywell, Inc.<br>Government and Aerospace<br>Products<br>ATTN: D.E. Broden/<br>MS MN50-2000<br>600 2nd Street NE<br>Hopkins, MN 55343 | 1                        | Olin Corporation<br>Smokeless Powder Operations<br>ATTN: V. McDonald<br>P.O. Box 222<br>St. Marks, FL 32355                                      |
| 1                        | Honeywell, Inc.<br>ATTN: R.E. Tompkins<br>MN38-3300<br>10400 Yellow Circle Drive<br>Minnetonka, MN 55343                                | 1                        | Paul Gough Associates, Inc.<br>ATTN: P.S. Gough<br>1048 South Street<br>Portsmouth, NH 03801-5423  |
| 1                        | IBM Corporation<br>ATTN: A.C. Tam<br>Research Division<br>5600 Cottle Road<br>San Jose, CA 95193  | 2                        | Princeton Combustion<br>Research Laboratories, Inc.<br>ATTN: M. Summerfield<br>N.A. Messina<br>475 US Highway One<br>Monmouth Junction, NJ 08852 |
| 1                        | IIT Research Institute<br>ATTN: R.F. Remaly<br>10 West 35th Street<br>Chicago, IL 60616   | 1                        | Hughes Aircraft Company<br>ATTN: T.E. Ward<br>8433 Fallbrook Avenue<br>Canoga Park, CA 91303   |

# DISTRIBUTION LIST

| <u>No. Of<br/>Copies</u> | <u>Organization</u>  | <u>No. Of<br/>Copies</u> | <u>Organization</u>  |
|--------------------------|--|--------------------------|--|
| 1                        | Rockwell International Corp.<br>Rocketdyne Division<br>ATTN: J.E. Flanagan/HB02<br>6633 Canoga Avenue<br>Canoga Park, CA 91304                       | 3                        | Thiokol Corporation<br>Wasatch Division<br>ATTN: S.J. Bennett<br>P.O. Box 524<br>Brigham City, UT 84302  |
| 4                        | Sandia National Laboratories<br>Combustion Sciences Dept.<br>ATTN: R. Cattolica<br>S. Johnston<br>P. Mattern<br>D. Stephenson<br>Livermore, CA 94550 | 1                        | United Technologies<br>ATTN: A.C. Eckbreth<br>East Hartford, CT 06108  |
| 1                        | Science Applications, Inc.<br>ATTN: R.B. Edelman<br>23146 Cumorah Crest<br>Woodland Hills, CA 91364  | 3                        | United Technologies Corp.<br>Chemical Systems Division<br>ATTN: R.S. Brown<br>T.D. Myers (2 copies)<br>P.O. Box 50015<br>San Jose, CA 95150-0015 |
| 1                        | Science Applications, Inc.<br>ATTN: H.S. Pergament<br>1100 State Road, Bldg. N<br>Princeton, NJ 08540  | 1                        | Universal Propulsion Company<br>ATTN: H.J. McSpadden<br>Black Canyon Stage 1<br>Box 1140<br>Phoenix, AZ 85029                                    |
| 3                        | SRI International<br>ATTN: G. Smith<br>D. Crosley<br>D. Golden<br>333 Ravenswood Avenue<br>Menlo Park, CA 94025                                      | 1                        | Veritay Technology, Inc.<br>ATTN: E.B. Fisher<br>4845 Millersport Highway<br>P.O. Box 305<br>East Amherst, NY 14051-0305                         |
| 1                        | Stevens Institute of Tech.<br>Davidson Laboratory<br>ATTN: R. McAlevy, III<br>Hoboken, NJ 07030  | 1                        | Brigham Young University<br>Dept. of Chemical Engineering<br>ATTN: M.W. Beckstead<br>Provo, UT 84601   |
| 1                        | Thiokol Corporation<br>Elkton Division<br>ATTN: W.N. Brundige<br>P.O. Box 241<br>Elkton, MD 21921  | 1                        | California Institute of Tech.<br>Jet Propulsion Laboratory<br>ATTN: MS 125/159<br>4800 Oak Grove Drive<br>Pasadena, CA 91103                     |
| 1                        | Thiokol Corporation<br>Huntsville Division<br>ATTN: R. Glick<br>Huntsville, AL 35807   | 1                        | California Institute of<br>Technology<br>ATTN: F.E.C. Culick/<br>MC 301-46<br>204 Karman Lab.<br>Pasadena, CA 91125                              |

# DISTRIBUTION LIST

| <u>No. Of<br/>Copies</u> | <u>Organization</u>  | <u>No. Of<br/>Copies</u> | <u>Organization</u>  |
|--------------------------|--|--------------------------|--|
| 1                        | University of California,<br>Berkeley<br>Mechanical Engineering Dept.<br>ATTN: J. Daily<br>Berkeley, CA 94720                    | 3                        | Georgia Institute of<br>Technology<br>School of Aerospace<br>Engineering<br>ATTN: E. Price<br>W.C. Strahle<br>B.T. Zinn<br>Atlanta, GA 30332 |
| 1                        | University of California<br>Los Alamos Scientific Lab.<br>P.O. Box 1663, Mail Stop B216<br>Los Alamos, NM 87545                  | 1                        | University of Illinois<br>Dept. of Mech. Eng.<br>ATTN: H. Krier<br>144MEB, 1206 W. Green St.<br>Urbana, IL 61801                             |
| 2                        | University of California,<br>Santa Barbara<br>Quantum Institute<br>ATTN: K. Schofield<br>M. Steinberg<br>Santa Barbara, CA 93106 | 1                        | Johns Hopkins University/APL<br>Chemical Propulsion<br>Information Agency<br>ATTN: T.W. Christian<br>Johns Hopkins Road<br>Laurel, MD 20707  |
| 2                        | University of Southern<br>California<br>Dept. of Chemistry<br>ATTN: S. Benson<br>C. Wittig<br>Los Angeles, CA 90007              | 1                        | University of Michigan<br>Gas Dynamics Lab<br>Aerospace Engineering Bldg.<br>ATTN: G.M. Faeth<br>Ann Arbor, MI 48109-2140                    |
| 1                        | Case Western Reserve Univ.<br>Div. of Aerospace Sciences<br>ATTN: J. Tien<br>Cleveland, OH 44135                                 | 1                        | University of Minnesota<br>Dept. of Mechanical<br>Engineering<br>ATTN: E. Fletcher<br>Minneapolis, MN 55455                                  |
| 1                        | Cornell University<br>Department of Chemistry<br>ATTN: T.A. Cool<br>Baker Laboratory<br>Ithaca, NY 14853                         | 3                        | Pennsylvania State University<br>Applied Research Laboratory<br>ATTN: K.K. Kuo<br>H. Palmer<br>M. Micci<br>University Park, PA 16802         |
| 1                        | Univ. of Dayton Rsch Inst.<br>ATTN: D. Campbell<br>AFRPL/PAP Stop 24<br>Edwards AFB, CA 93523                                    | 1                        | Pennsylvania State University<br>Dept. of Mechanical Engineering<br>ATTN: V. Yang<br>University Park, PA 16802                               |
| 1                        | University of Florida<br>Dept. of Chemistry<br>ATTN: J. Winefordner<br>Gainesville, FL 32611                                     |                          |  |

# DISTRIBUTION LIST

| <u>No. Of<br/>Copies</u> | <u>Organization</u>   | <u>No. Of<br/>Copies</u> | <u>Organization</u>   |
|--------------------------|---|--------------------------|---|
| 1                        | Polytechnic Institute of NY<br>Graduate Center<br>ATTN: S. Lederman<br>Route 110<br>Farmingdale, NY 11735   | 1                        | University of Texas<br>Dept. of Chemistry<br>ATTN: W. Gardiner<br>Austin, TX 78712  |
| 2                        | Princeton University<br>Forrestal Campus Library<br>ATTN: K. Brezinsky<br>I. Glassman<br>P.O. Box 710<br>Princeton, NJ 08540                        | 1                        | University of Utah<br>Dept. of Chemical Engineering<br>ATTN: G. Flandro<br>Salt Lake City, UT 84112   |
| 1                        | Princeton University<br>MAE Dept.<br>ATTN: F.A. Williams<br>Princeton, NJ 08544   | 1                        | Virginia Polytechnic<br>Institute and<br>State University<br>ATTN: J.A. Schetz<br>Blacksburg, VA 24061  |
| 1                        | Purdue University<br>School of Aeronautics<br>and Astronautics<br>ATTN: J.R. Osborn<br>Grissom Hall<br>West Lafayette, IN 47906                     | 1                        | Commandant<br>USAFAS<br>ATTN: ATSF-TSM-CN<br>Fort Sill, OK 73503-5600   |
| 1                        | Purdue University<br>Department of Chemistry<br>ATTN: E. Grant<br>West Lafayette, IN 47906  | 1                        | F.J. Seiler Research Lab (AFSC)<br>ATTN: S.A. Shakelford<br>USAF Academy, CO 80840-6528   |
| 2                        | Purdue University<br>School of Mechanical<br>Engineering<br>ATTN: N.M. Laurendeau<br>S.N.B. Murthy<br>TSPC Chaffee Hall<br>West Lafayette, IN 47906 | 1                        | Freedman Associates<br>ATTN: E. Freedman<br>2411 Diana Road<br>Baltimore, MD 21209-1525   |
| 1                        | Rensselaer Polytechnic Inst.<br>Dept. of Chemical Engineering<br>ATTN: A. Fontijn<br>Troy, NY 12181   |                          | <u>Aberdeen Proving Ground</u><br><br>Dir, USAMSAA<br>ATTN: AMXSY-D<br>AMXSY-MP, H. Cohen<br>Cdr, USATECOM<br>ATTN: AMSTE-TO-F<br>Cdr, CRDEC, AMCCOM<br>ATTN: SMCCR-RSP-A<br>SMCCR-MU<br>SMCCR-SPS-IL |
| 1                        | Stanford University<br>Dept. of Mechanical<br>Engineering<br>ATTN: R. Hanson<br>Stanford, CA 94305  |                          |   |

USER EVALUATION SHEET/CHANGE OF ADDRESS

This laboratory undertakes a continuing effort to improve the quality of the reports it publishes. Your comments/answers below will aid us in our efforts.

1. Does this report satisfy a need? (Comment on purpose, related project, or other area of interest for which the report will be used.) \_\_\_\_\_  
\_\_\_\_\_
2. How, specifically, is the report being used? (Information source, design data, procedure, source of ideas, etc.) \_\_\_\_\_  
\_\_\_\_\_
3. Has the information in this report led to any quantitative savings as far as man-hours or dollars saved, operating costs avoided, or efficiencies achieved, etc? If so, please elaborate. \_\_\_\_\_  
\_\_\_\_\_
4. General Comments. What do you think should be changed to improve future reports? (Indicate changes to organization, technical content, format, etc.) \_\_\_\_\_  
\_\_\_\_\_

BRL Report Number \_\_\_\_\_ Division Symbol \_\_\_\_\_

Check here if desire to be removed from distribution list. \_\_\_\_\_

Check here for address change. \_\_\_\_\_

Current address: Organization \_\_\_\_\_  
Address \_\_\_\_\_  
\_\_\_\_\_

-----FOLD AND TAPE CLOSED-----

Director  
U.S. Army Ballistic Research Laboratory  
ATTN: SLCBR-DD-T (NEI)  
Aberdeen Proving Ground, MD 21005-5066

OFFICIAL BUSINESS  
PENALTY FOR PRIVATE USE \$300



NO POSTAGE  
NECESSARY  
IF MAILED  
IN THE  
UNITED STATES

Director  
U.S. Army Ballistic Research Laboratory  
ATTN: SLCBR-DD-T (NEI)  
Aberdeen Proving Ground, MD 21005-9989